Synthesis and Characterization of Poly(γ-methacryloxypropyltrimethoxysilane)-Grafted Silica Hybrid Nanoparticles Prepared by Surface-Initiated Atom Transfer Radical Polymerization

Ji-Rong Wu,[1] Guo-Qiao Lai,[1] Hai-Jiang Yu,[2] Zheng-Hong Luo[2]

[1]*Key Laboratory of Organosilicon Chemistry and Material Technology of Ministry of Education, Hangzhou Normal University, Hangzhou 310012, People's Republic of China*
[2]*Department of Chemical and Biochemical Engineering, College of Chemistry and Chemical Engineering, Xiamen University, Xiamen 361005, People's Republic of China*

Received 10 May 2011; accepted 11 August 2011
DOI 10.1002/app.35469
Published online 23 November 2011 in Wiley Online Library (wileyonlinelibrary.com).

ABSTRACT: Poly(γ-methacryloxypropyltrimethoxysilane) (PMPTS)-grafted silica hybrid nanoparticles were prepared by surface-initiated atom transfer radical polymerization (SI-ATRP). The resulting PMPTS-grafted silica hybrid nanoparticles were characterized using Fourier transform infrared spectroscopy (FTIRS), nuclear magnetic resonance (NMR), gel permeation chromatography (GPC), X-ray photoelectron spectroscopy (XPS), atomic force microscopy (AFM), scanning electron microscopy (SEM), static water contact angle (WCA) measurement, and thermogravimetric analysis (TGA). Combined FTIRS, NMR, XPS, SEM, and TGA studies confirmed that these hybrid nanoparticles were successfully prepared by surface-initiated ATRP. SEM and AFM studies revealed that the surfaces of the nanoparticles were rough at the nanoscale. In addition, the results of the static WCA measurements showed that the nanoparticles are of low surface energy and their surface energy reaches as low as 6.10 mN m^{-1}. © 2011 Wiley Periodicals, Inc. J Appl Polym Sci 124: 3821–3830, 2012

Key words: SI-ATRP; PMPTS-grafted silica hybrid nanoparticles; low surface energy

INTRODUCTION

Organic/inorganic hybrid nanoparticles have attracted ever-increasing attention due to their intriguing properties associated with inorganic cores (optical, magnetic, and mechanical properties, etc.) and polymeric shells (processability, compatibility, stimuli-responsiveness, etc.).[1–4] Hybrid nanoparticles using silica (SiO_2) particles as substrates can handle better the unusual properties of nanoparticles (optical, electronic, catalytic, etc.) due to the controllable distance of interparticle by the polymer grafted onto them and are one important family of them.[5] There are many ways to prepare these hybrid nanoparticles, such as direct blend,[6–8] sol–gel method,[9–12] and grafting technique.[13–18] Grafting technique involves either the "grafting from"[13–17] or the "grafting to" approaches.[18–20] Compared with "grafting to", the "grafting from" approach provides much better control over surface grafting densities and grafted chain lengths, taking advantage of the field of controlled/living radical polymerization, such as atom transfer radical polymerization (ATRP),[21–25] reversible addition–fragmentation chain transfer polymerization (RAFT),[26] and nitroxide-mediated radical polymerization (NMRP).[27,28] Among these controlled/living radical surface-initiated polymerization approaches, the surface-initiated ATRP (SI-ATRP) has become the most popular route due to its tolerance to a wide range of functional monomers and less stringent polymerization conditions.

Recently, many hybrid nanoparticles using SiO_2 particles as substrates were prepared by the SI-ATRP.[29–34] Patten and coworkers prepared hybrid nanoparticles using the SI-ATRP for styrene or methyl methacrylate from silica nanoparticles.[29,30] Li et al. reported the preparation of poly(methoxytri(ethylene glycol) methacrylate)-grafted SiO_2 hybrid nanoparticles.[31] Chen et al. synthesized a range of

Correspondence to: Z.-H. Luo (luozh@xmu.edu.cn).
Contract grant sponsor: National Natural Science Foundation of China; contract grant number: 20406016.
Contract grant sponsor: Nation Defense Key Laboratory of Ocean Corrosion and Anti-corrosion of China; contract grant number: 51449020205QT8703.
Contract grant sponsor: Fujian Province Science and Technology Office of China; contract grant number: 2005H040.

polyelectrolyte-grafted SiO_2 particles by grafting suitable initiators onto silica particles followed by surface-initiated ATRP.[32] However, in the past, less attention has been paid to the preparation of organsilicone polymers-grafted SiO_2 hybrid nanoparticles. Siloxane polymers are highly flexible, giving them a low glass transition temperature (T_g), high dielectric strength, low surface tension and energy, high gas permeability,[33] and thermal and oxidative stability. Unfortunately, the mechanical and resistance properties of siloxane polymers to organic solvents, acids, and bases are poor.[33] Recently, increasing attention has been paid to the combined incorporation of siloxane moieties and inorganic nanoparticles into synthetic materials, i.e., organic/inorganic hybrid nanoparticles. The comprehensive properties of these materials which possess advantages from both siloxane and inorganic nanoparticles are better. On the other hand, among the family of siloxane polymers, poly(γ-methacryloxypropyltrimethoxysilane) (PMPTS) is a hydrophobic organsilicone polymer[33] and silica/PMPTS may be an excellent superhydrophobic material (this is the purpose for grafting PMPTS onto SiO_2 nanoparticles). More recently, our group synthesized silica/polystyrene (SiO_2/PS) and silica/polystyrene-*b*-PMPTS (SiO_2/PS-*b*-PMPTS) hybrid nanoparticles via SI-ATRP.[34] Their wettabilities were measured and compared by means of water contact angle (WCA) and surface roughness. Our previous work only aimed at the comparison of their wettabilities and was open as a communication; the structure and surface behavior of the above hybrid nanoparticles were not systemically investigated. In addition, in our previous work,[34] we found that the static WCA of SiO_2/polystyrene (PS)-*b*-PMPTS hybrid nanoparticles is smaller than that of SiO_2/PS hybrid nanoparticles, which shows that the combination and competition of surface chemistry and roughness of a solid material can finally determine its wettability. However, it is well known that the static WCA of PMPTS is higher than that of PS. Therefore, it is necessary to investigate the wettability of SiO_2/PMPTS. PMPTS employed to prepare hybrid nanoparticles has not been reported.[34]

In the present work, we focus on the improvement of the hydrophobic properties given by the inclusion of silica nanoparticles in the PMPTS matrix by surface-initiated ATRP to obtain a relatively high hydrophobic film with rough surface at the nanoscale. The grafting of polymer chains onto the particles will serve to improve the compatibility between the SiO_2 particles and the PMPTS matrix. Although PMPTS is not very hydrophobic, we generate a relatively high hydrophobic film with rough surface at the nanoscale using PMPTS.

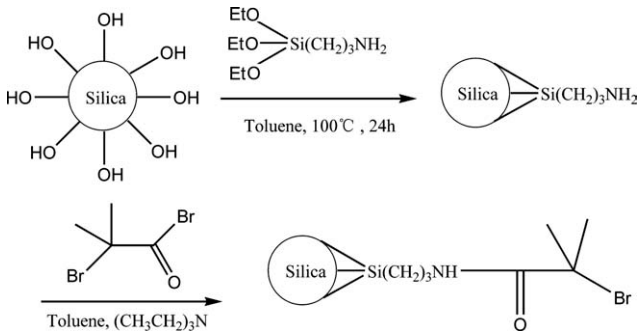

Scheme 1 The two-step process of immobilization of the surface initiators by grafting of APTS and 2-bromoisobutyryl bromide onto the surface of the silica nanoparticles.

EXPERIMENTAL

Materials

(3-Aminopropyl)triethoxysilane (APTS, 98%) was provided by Alfa Aesar (Massachusetts, USA). γ-Methacryloxypropyltrimethoxysilane (MPTS, 98%) and 2-bromoisobutyrate bromide (98%) were obtained from A Better Choice for Research Chemicals GmbH & Co. KG (ABCR, Hamburg, Germany). SiO_2 nanoparticles, 1,1,4,7,7-pentamethyldiethylenetriamine (PMDETA, 98%) and copper (I) bromide (98%, stored under nitrogen) were supplied by Aldrich (Missouri, USA). The SiO_2 used in this study has a specific surface area of 200 ± 25 m^2 g^{-1} and a mean particle diameter of 14 nm. Copper (I) bromide was purified to remove Cu (II) by precipitation from the corresponding concentrated acid by addition of water under nitrogen atmosphere.

Immobilization of the initiator on the surface of silica

A two-step process shown in Scheme 1 was used to immobilizate the surface initiators as previously reported.[35,36]

Synthesis of PMPTS-grafted silica hybrid nanoparticles

PMPTS-grafted SiO_2 hybrid nanoparticles (SiO_2/PMPTS) were synthesized by polymerizing MPTS from the surface of SiO_2-APTS-Br initiator (Scheme 2). A typical example of grafting polymerization was as follows:

The initiator-modified SiO_2 particles (SiO_2-APTS-Br) (67 mg, 0.095 mmol), CuBr (14 mg, 0.095 mmol), the deactivator $CuBr_2$ (14 mg, 0.095 mmol), and dry toluene (2 mL) were added to a dried round-bottom flask and sealed with a rubber septum. The flask was degassed and backfilled with nitrogen three times and kept under a nitrogen atmosphere. Then the monomer MPTS (2.26 mL, 9.5 mmol) was charged into the flask and the mixture was

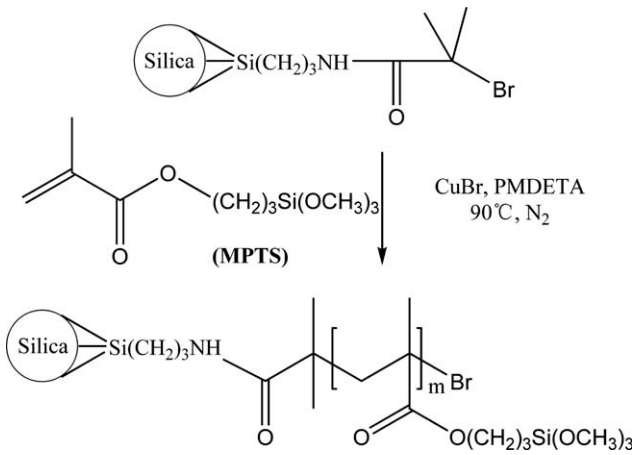

Scheme 2 Schematic formation of SiO_2/PMPTS hybrid nanocomposites by surface initiated ATRP.

evacuated and flushed with nitrogen three times to remove oxygen. SiO_2 particles were dispersed by ultrasonication before heating. PMDETA (20 μL, 0.095 mmol) was added into the flask to afford the CuBr/PMDETA/SiO_2-APTS-Br/MPTS molar ratio of 1 : 1 : 1 : 100. The reaction mixture was stirred until it became homogeneous. The polymerization was performed at 90–100°C for 6 h. To remove free polymers, the product was washed with tetrahydrofuran (THF) and centrifuged at 4000 rpm to isolate the PMPTS-grafted silica nanoparticles (yield: 2.0 g, 82%).

Characterization

Thermogravimetric analysis (TGA) was performed to determine the surface density of the hydroxyls on the surface of SiO_2 nanoparticles on a SDT Q600 simultaneous DSC-TGA instrument, at a scan rate of 10 °C min^{-1}, from room temperature to 1200°C under nitrogen. The amount of polymer grafted onto the nano-SiO_2 surface was also determined by TGA. Sample was heated to 700°C from room temperature at a speed of 10 °C min^{-1} under nitrogen.

The elemental analyses were performed by a varioEL III analyzer. Fourier transform infrared (FTIR) spectra of the pristine and modified silica particles were recorded from KBr pellets on an Avatar 360 FTIR spectrophotometer (Nicolet).

Polymer/SiO_2 hybrid nanoparticles were etched by hydrofluoric acid (HF), and the cleaved polymer was measured by nuclear magnetic resonance (^{1}H NMR) on a Bruker AV400 NMR spectrometer in deuterated chloroform.

The number average molecular weights (M_n) and molecular weight distribution (M_w/M_n) of the cleaved polymer of PMPTS were determined at 40°C by gel permeation chromatography (GPC) equipped with a waters 1515 isocratic HPLC pump, three Styragel columns (Waters HT4, HT5E, and HT6) and a waters 2414 refractive index detector (set at 30°C), using THF as the eluent at a flow rate of 1.0 mL min^{-1}. A series of poly(methyl methacrylate) narrow-standards were employed to generate a universal calibration curve.

X-ray photoelectron spectroscopy (XPS) spectra were recorded to determine the surface composition of PMPTS-grafted SiO_2 particles using a PHI quantum 2000 scanning ESCA microprobe (Physical Electronic, Minnesota, USA), equipped with an Al $K\alpha_{1,2}$ monochromatic source of 1486.60 eV.

The morphology of the pristine, modified, and grafted silica particles was observed using a scanning electron microscope (SEM) (S-4800).

Atomic force microscopy (AFM) observation was made on a 5500ILM Atomic Force Microscope (Agilent, Beijing, China) in the tapping mode to measure the film surface roughness.

Static WCAs of the PMPTS-grafted silica hybrid nanoparticle films were measured by casting a 3 wt % THF suspension on glass slides and were recorded on a telescopic goniometer (SL-200B). For each angle reported, at least seven readings from different surface locations were averaged.

Preparations of the films based on SiO_2/PMPTS nanoparticles

A suspension of 1% (w/w) nanoparticles in THF was slowly cast on a cleaned glass slide. The suspension was evaporated at room temperature under a nearly saturated vapor of THF over 3 days. The formed film was further dried under vacuum for 6–8 h.

RESULTS AND DISCUSSION

Synthesis and characterization of the SiO_2 nanoparticle initiator

To quantify the amount of APTS required for grafting, it is necessary to determine the surface density

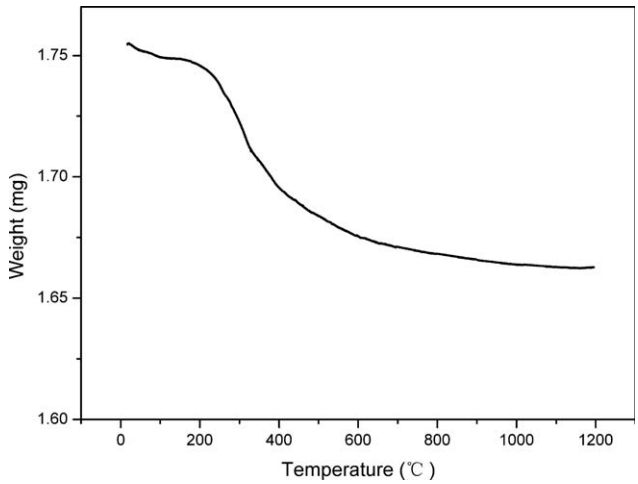

Figure 1 TGA curve of SiO_2 microspheres.

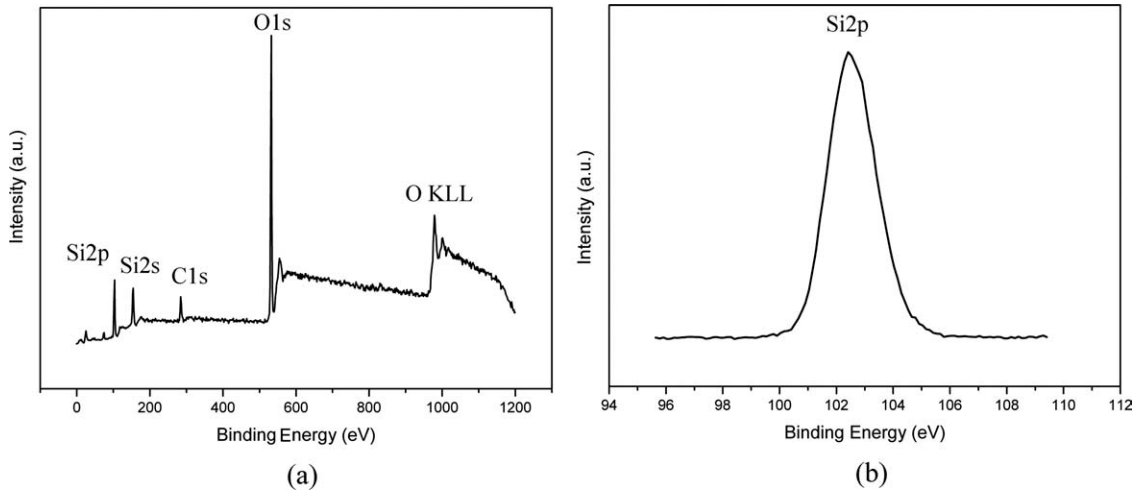

Figure 2 XPS spectra of pristine SiO_2: (a) the survey scan spectrum and (b) the Si2p spectrum.

of the hydroxyls on the SiO_2 nanoparticles. TGA was used in the present study (Fig. 1). According to the report by Ek et al.,[37] we can determine that the mole of hydroxyls left per gram of SiO_2 is 4.68 mmol g^{-1} SiO_2.

APTS contains a hydrolyzable alkoxy group which can readily react with silanol groups on silica.[38,39] Simultaneously, the primary amino groups which can react with 2-bromoisobutyrate bromide are introduced onto particle surface as shown in Scheme 1. Elemental analyzer was used to analyze the presence of amino group on the surface of SiO_2. The elemental analysis result also shows that the concentration of amino groups on the surface was about 1.88 mmol g^{-1} SiO_2, which enhances the compatibility of the modified SiO_2 as organic–inorganic filler in nano-size with organic matrix, e.g., polymers.[40] ATRP-initiator-anchored SiO_2 particles were prepared after a reaction of aminated SiO_2 particles with 2-bromoisobutyryl bromide. The elemental analysis result shows that the concentration of bromo-ester on the surface is about 1.43 mmol g^{-1} SiO_2.

To confirm the immobilization of the initiator on the surface of SiO_2, the surface of SiO_2 was characterized with XPS (Figs. 2–4). Table I shows the XPS atomic concentration of C 1s, O 1s, Si 2p, N 1s, and Br 3d of the respective substrate surface. The atomic percentage of the elements concerned was calculated by dividing the peak area by the sensitivity factor and expressed as a fraction of the summation of all normalized intensities:

$$[\mathrm{A}]\mathrm{atomic}\% = \{(I_\mathrm{A}/F_\mathrm{A})/\sum(I/F)\} \times 100\%. \quad (1)$$

where, I and F are the intensity and sensitivity factor, respectively.[41]

The spectra of SiO_2-APTS (Fig. 3) and SiO_2-APTS-Br (Fig. 4) showed the similar signals as that of pristine SiO_2 (Fig. 2), but the relative integral ratio of

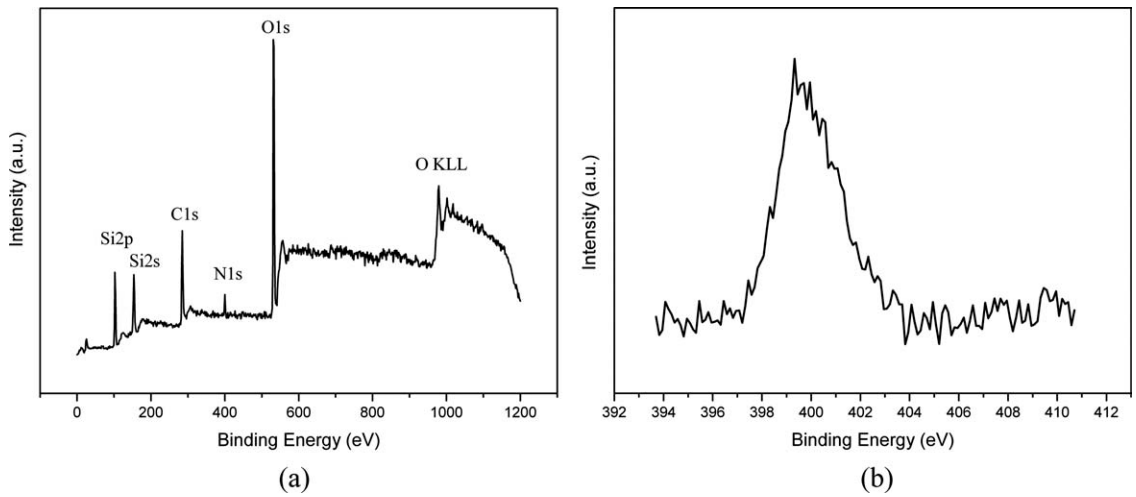

Figure 3 XPS spectra of SiO_2-APTS: (a) the survey scan spectrum and (b) the N1s spectrum.

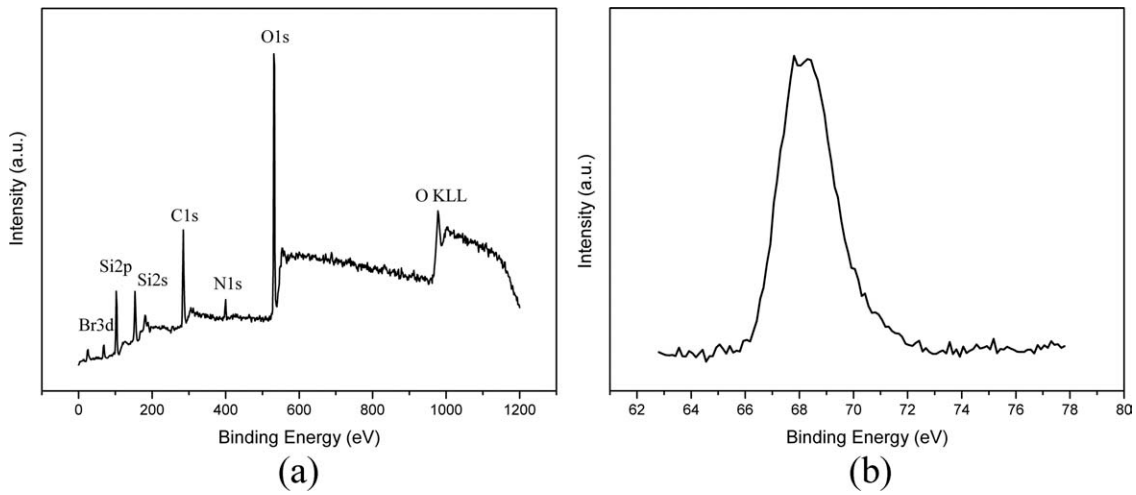

Figure 4 XPS spectra of SiO_2-APTS-Br: (a) the survey scan spectrum and (b) the Br3d spectrum.

carbon signals was slightly higher, and the small signals of nitrogen from SiO_2-APTS (Fig. 3) and bromine from SiO_2-APTS-Br (Fig. 4) were also observed, respectively. Therefore, the immobilization of the bromoester initiator on the surface of SiO_2 nanoparticles was successful.

Synthesis and characterization of SiO_2/PMPTS hybrid nanoparticles

From Figure 5(a), the absorption bands based on imide O=C—NH linkage at 1645 cm^{-1}, Si—O—Si band at 1110 cm^{-1} and Si—CH_3 band at 805 cm^{-1} could be observed, indicating that the SiO_2/APTS-Br macroinitiator was synthesized. In FTIR spectra of SiO_2/PMPTS samples [Fig. 5(b)], the typical vibrations of the organic components of the matrix are evident. In particular, the sharp band of the O—C=O ester group from MPTS is clearly detected at 1730 cm^{-1}. And absorptions at 2949 cm^{-1} and 2842 cm^{-1} are attributed to the stretching vibration modes of –CH_3 and –CH_2 groups from PMPTS, respectively. In FTIR spectra of SiO_2/PMPTS nanoparticle samples, the characteristic bands of PMPTS at 1730 cm^{-1} (ester band) and 2949 cm^{-1}, 2842 cm^{-1} (C—H bands) indicate the formation of hybrid nanoparticles through the polymerization reactions, which are initiated by silica surface groups (-Br).

As mentioned in the literature,[42] because of the presence of the reactive trimethoxysilyl group, γ-MPTS is sensitive to self-condensation and should be carefully manipulated. For example, removing the inhibitor (monomethyl ether, 4-methoxyphenol (MEHQ)) present in the commercial monomer by filtration through an activated basic alumina column would lead to an instantaneous condensation of the liquid monomer onto the column. Therefore, the purification was performed by distillation (120°C, 0.1 mmHg) under argon and reduced pressure. Since these harsh conditions may have degraded the monomer, the recovered product, stored at 4°C in a Schlenk tube under argon, was analyzed by ^{1}H-NMR spectroscopy (Fig. 6). The calculated ratio of the methoxy protons (6 at 3.58 ppm) and rest of the protons of the molecule is in agreement with a successful purification without any condensation of the trimethoxysilyl functions.[43]

The SiO_2 cores of SiO_2/MPTS were completely etched by HF and then the cleaved PMPTS polymer was characterized by ^{1}H NMR, as shown in Figure 7, which reveals the presence of the characteristic signals of PMPTS at δ = 4.19 ppm (3), 3.99 ppm (3), and 0.9 ppm (5). The above observations prove the successful synthesis of the PMPTS grafted SiO_2.

TABLE I
XPS Quantification of SiO_2, SiO_2-APTS, and SiO_2-APTS-Br Surface in Atomic % (Normalized to 100)

Sample	C 1s (%)	O 1s (%)	Si 2p (%)	N 1s (%)	Br 3d (%)
Pristine SiO_2 surface	10.7	66.6	23.7		
SiO_2-APTS surface	32	47.1	17.4	3.5	
SiO_2-APTS-Br surface	36.1	41.8	17.0	3.3	1.8

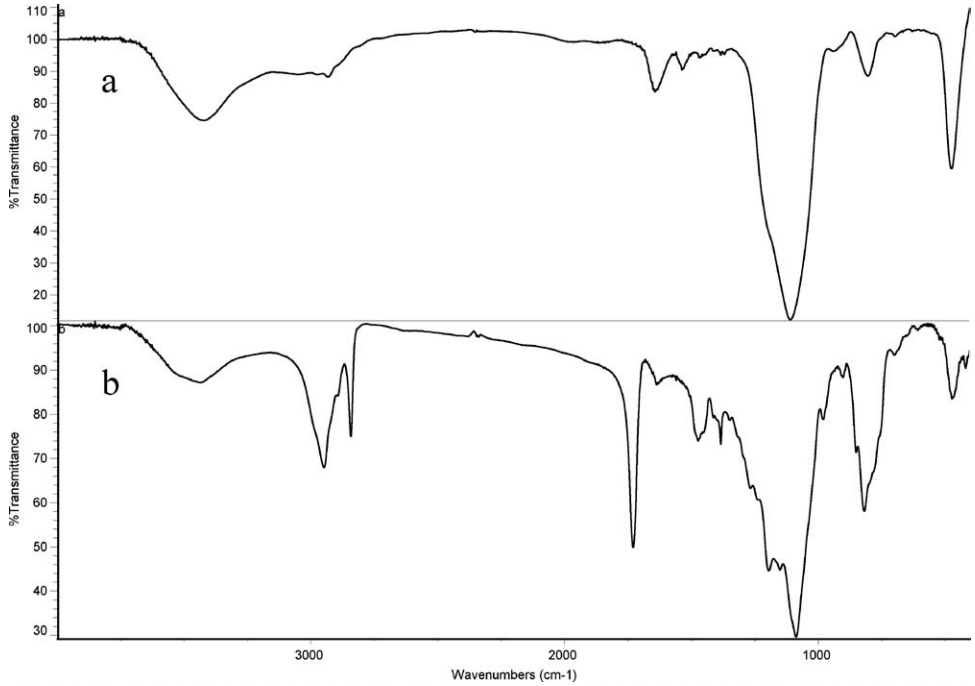

Figure 5 FTIR spectra of (a) SiO_2-APTS-Br, (b) SiO_2/PMPTS (tethered PMPTS brush).

Molecular weights (M_w and M_n) and polydispersity index

The molecular weight and molecular weight distribution of PMPTS were determined by GPC using THF as the eluent. GPC analysis in THF revealed a mono-modal peak with a M_n of 24,800 and a polydispersity index (PDI), M_w/M_n, of 1.31 (Fig. 8). The elution peak of PMPTS is slightly asymmetric and exhibits no apparent tailing at the lower molecular weight side.

XPS investigation

XPS was carried out to determine the surface chemical composition of nanoparticle film. By comparing the relative integral ratios of the signals, silicon is less in SiO_2/PMPTS (Fig. 9) than in the pristine silica (Fig. 2), SiO_2-APTS (Fig. 3), and SiO_2-APTS-Br (Fig. 4), while the ratio of carbon is more in SiO_2/PMPTS. The content of elements (C, O, and Si) on the surface layer of the PMPTS grafted nano-SiO_2 is 66.33%, 26.63%, and 7.04%, respectively. On comparing C/Si atom ratio in Table I, the sharp change of C/Si atom ratio is almost the same as that in PMPTS, suggesting that SiO_2 particles were encapsulated and shielded by PMPTS layer. The survey and C 1s spectra given in Figure 9 showed the presence of groups of Si—O that was introduced by PMPTS. The C 1s spectrum consists of a complex pattern of peaks which stand for two kinds of carbon bonds: the peak at 289.0 eV can be attributed to —C=O, and the peak at 284.8 eV (reference peak) to alkyl carbon (C—C) [Fig. 9(b)]. The O 1s spectrum presents a peak at 533.25 eV that is identified as the O 1s in PMPTS. The weak peak of Si 2p appears at 102.4 eV, in agreement with Si 2p for Si—O, corresponding to Si 2p in PMPTS. From the results above, it can be concluded that PMPTS is attached to SiO_2 nanoparticles via chemical bond to form the composite nanoparticles with a core of SiO_2 and the surface layer of PMPTS.

Scanning electron microscopy

Figure 10 shows SEM micrographs of the SiO_2 particles before and after the surface-initiated ATRP

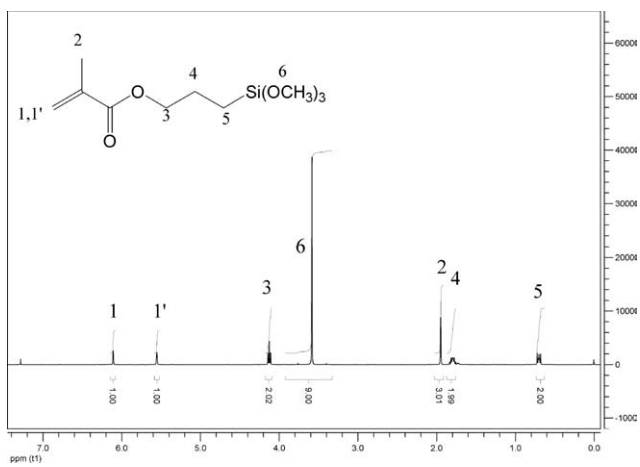

Figure 6 ^{1}H-NMR spectrum of distillated MPTS (deuterated chloroform, number of scans 16).

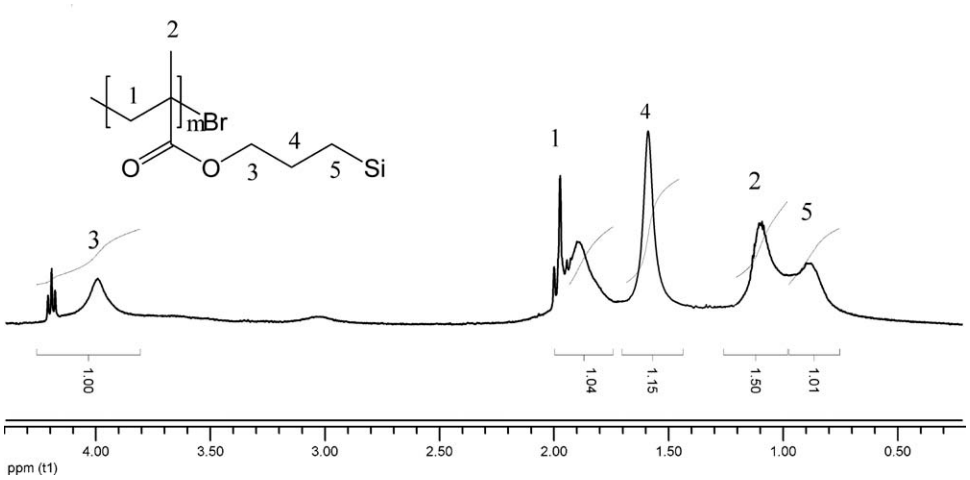

Figure 7 ^{1}H-NMR spectra of cleaved SiO_2/PMPTS nanocomposite in $CDCl_3$.

polymerization of MPTS. In Figure 10(a), the pristine silica particles are spherical and nothing can be seen among the particles. Its diameter was about 14 nm. In fact, the primary nanoparticles are strongly aggregated in a dry state. The significant small spherical silica particles aggregate was clearly observed from SEM image as shown in Figure 10(a). The morphology of modified silica is also characterized by the SEM and presented in Figure 10(b,c). The SEM images of the aminopropyl end-capped silica particles [Fig. 10(b)] and α-bromoester end-capped silica particles [Fig. 10(c)] do not show much significant difference in the morphology from that of the pristine silica except the change in the particle size because of molecular layers loading onto the silica surface with the long carbon chains outside. It is clear from the photographs that the covalent immobilization of the initiator on the silica surface [Fig. 10(b,c)] slightly incremented the silica particle size. On comparing Figure 10(b,c) with Figure 10(a), it can be found that the diameter of the particle became bigger, suggesting there is fair content of molecular layers on the silica surface. Interestingly, grafting of MPTS [Fig. 10(d)] made the particles' surface become rough and unclear, suggesting that each silica particle aggregate was coated with an outer layer of PMPTS chains. Furthermore, the long polymer chains twisted each other, which led to the further aggregation of the silica particles.

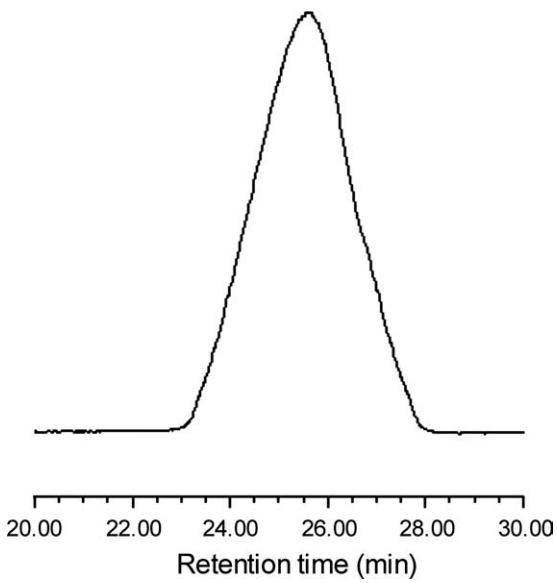

Figure 8 GPC traces of PMPTS (M_n = 24,860, M_w/M_n = 1.31).

Calculation of surface density of PMPTS

The grafting density of PMPTS on SiO_2 surface was estimated from TGA data (Fig. 11) and molecular weight of polymer as follows[44]:

$$\text{SurfacedensityofPMPTS} = \frac{\frac{W_{\text{PMPTS}}}{100-W_{\text{PMPTS}}} \times 100 - W_{\text{SiO}_2}}{M_{\text{PMPTS}} \times S_{\text{spe}} \times 100}, \quad (2)$$

where, W_{PMPTS} is the weight loss percentage corresponding to the decomposition of the PMPTS chains (57.0), W_{SiO_2} is the residual weight percentage (4.8), M_{PMPTS} is the molecular weight of the PMPTS chain (24,800 g mol^{-1}), and S_{spe} is the specific surface area of silica (200 m^2 g^{-1}). From Figure 11, one knows that the mass loss for the modified curve is significant only above 300°C while in the pristine powders significant mass loss occurs below 200°C (due to water loss by adsorbing). The polymer content of SiO_2/PMPTS was estimated by weight loss of TGA. The TGA of SiO_2/PMPTS [Fig. 11(b)] showed the onset decomposition temperature (T_d) at 421.8°C and the weight loss of 57.0% at 700°C. The T_d is in agreement with that of the polymer PMPTS, indicating that the weight loss was originated from grafted PMPTS on the silica surface. In comparison with the weight loss of 4.8% of pristine silica between 200

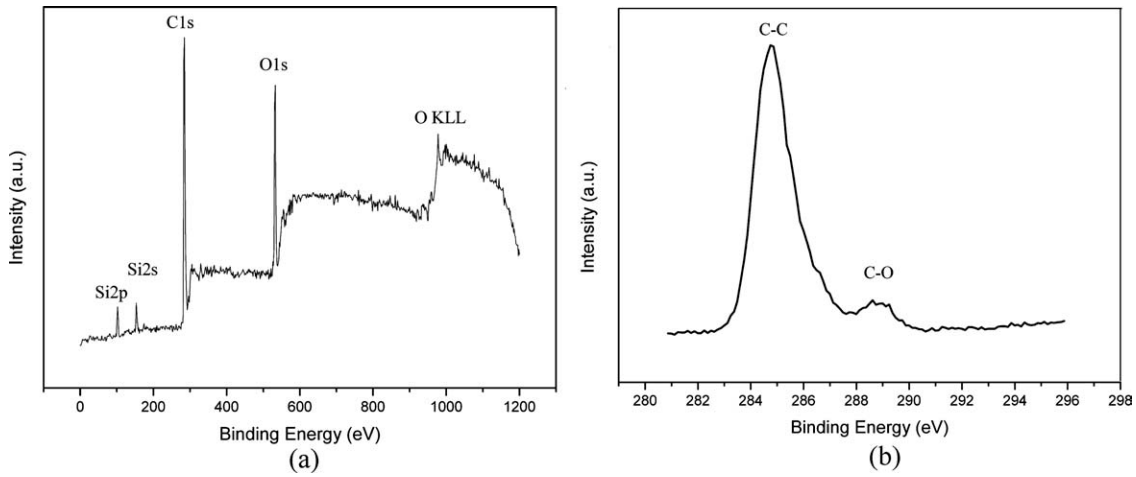

Figure 9 XPS spectrum of SiO_2/PMPTS: (a) the survey scan spectrum and (b) the C1s spectrum.

and 1200°C [Fig. 11(a)], the polymer content of SiO_2/PMPTS is 52.2 of total amount. Thus, the surface grafting density of PMPTS was calculated to be about 0.26 μmol m^{-2}.

Atomic force microscope and contact angle measurement

To obtain the morphology and surface roughness of the PMPTS-grafted SiO_2 particles, we imaged the surface of the films using AFM (Fig. 12). As seen in the image, the surface texture and the average size of the features were consistent with inorganic particles coated with polymer as observed in the SEM images. In addition, we can also obtain the following data via using the software along with 5500ILM Atomic Force Microscope. The average height of the protuberant area in Figure 12 is 36 nm, the size of the discontinuous phase area is about 30–50 nm, and root mean square (RMS) roughness (R_q) in an area of 1 μm^2 of this sample is 5.23 nm. The average roughness (R_a) was estimated to be 4.16 nm over a scope of 1 μm^2.

The presence of the hydrophobic monomer in the final material has been detected. The WCA was used to investigate the hydrophobicity on the surface of the hybrid film by introducing the hydrophobic monomer. As evident from Figure 10(d), the static-WCA is

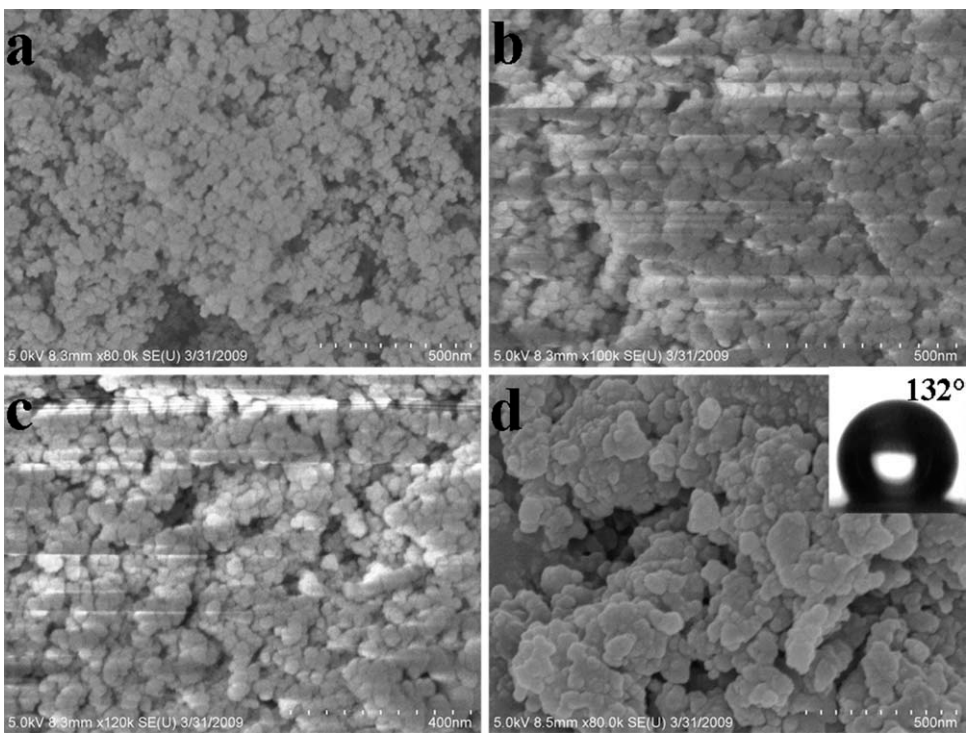

Figure 10 SEM images of (a) pristine silica, (b) SiO_2-APTS, (c) SiO_2-APTS-Br and (d) SiO_2/PMPTS, pictured with images (inset) of the corresponding WCA.

characteristic of hydrophobic nanoparticles. Usually, contact angle analysis provides a quick and simple means of assessing the reactivity of the surface and allows for general comparisons providing a qualitative test. However surface roughness can also influence the contact angle results.[45] Therefore, we measured the contact angle and roughness simultaneously from the same set of samples. The contact angles were taken within 20 s after formation of the sessile drop. After each cleaning step, the roughness of the surfaces was detected by AFM. The roughness of the surfaces was quantified by using the RMS value R_q which represents the root mean square average of height deviations Z_i taken from the mean data plane [eq. (3)][45]:

$$R_q = \sqrt{\frac{\sum Z_i^2}{n}} \tag{3}$$

When R_q is 5.23 nm, the WCAs toward the air-side surface of the SiO_2/PMPTS films can reach as high as 132° [Fig. 10(d)]. Contact angle measurement strongly implies that the SiO_2/PMPTS nanoparticles create hydrophobic films. The PMPTS polymer layer on the surface of silica with high contact angle is interesting in the study on hydrophobic materials.

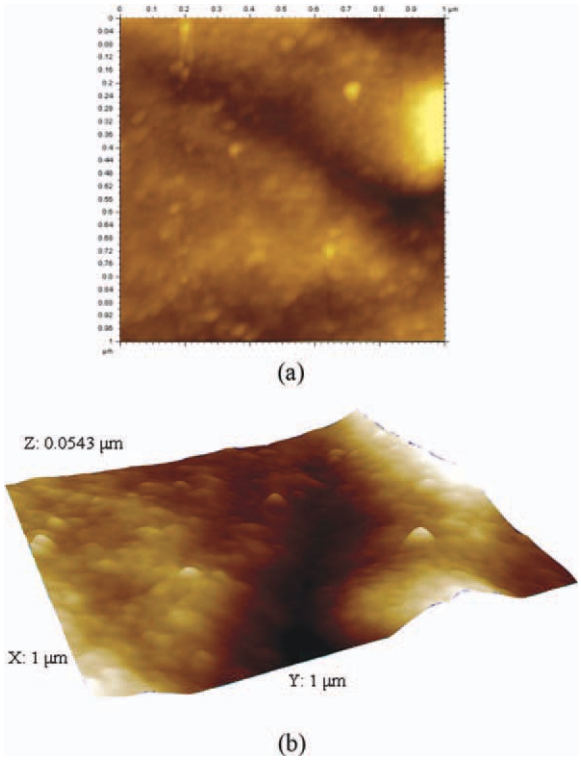

Figure 12 Tapping mode AFM images of PMPTS-grafted SiO_2 nanoparticles. [Color figure can be viewed in the online issue, which is available at wileyonlinelibrary.com.]

CONCLUSIONS

Well-defined SiO_2/PMPTS hybrid nanoparticles are successfully prepared via surface-initiated ATRP confirmed by FTIR, NMR, XPS, SEM, and TGA studies. The polymerization occurs in a mild reaction condition with the molecular weight measured by GPC as predicted. SEM and AFM images showed the rough nanostructures of the SiO_2/PMPTS nanoparticles. The analysis of contact angle shows that the SiO_2/PMPTS nanoparticles exhibit good water repellence with hydrophobic surface. This study provides a generally applicable approach to the preparation of hydrophobic inorganic–organic nanoparticles initiated by the inorganic SiO_2 initiator.

Authors thank Professor Bing-Wei Mao (State Key Laboratory for Physical Chemistry of Solid Surfaces and Department of Chemistry, College of Chemistry and Chemical Engineering, Xiamen University) for AFM analysis.

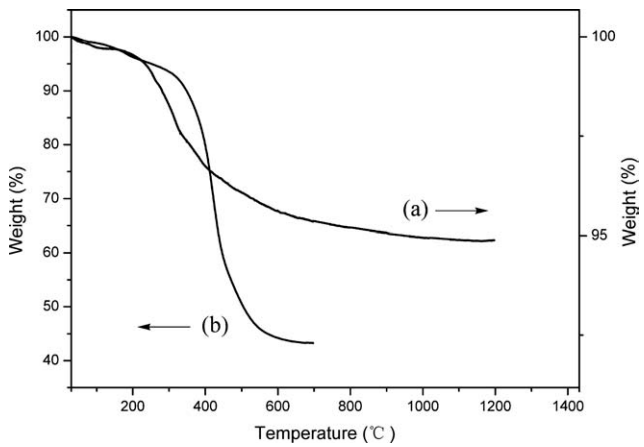

Figure 11 TGA curve of (a) SiO_2 microspheres and (b) SiO_2/PMPTS.

References

1. Hawker, C. J.; Wooley, K. L. Science 2005, 309, 1200.
2. Chen, T.; Colver, P. J.; Bon, S. A. F. Adv Mater 2007, 19, 2286.
3. Zhang, H.; Wang, C. L.; Li, M. J.; Zhang, J. H.; Lu, G.; Yang, B. Adv Mater 2005, 17, 853.
4. Zhang, Y. F.; Gu, W. Y.; Xu, H. X.; Liu, S. Y. J. Polym Sci Part A: Polym Chem 2008, 46, 2379.
5. Merikhi, J.; Feldmann, C. J Colloid Interface Sci 2000, 228, 121.
6. Hong, J. I.; Cho, K. S.; Chung, C. I.; Schadler, L. S.; Siegel, R. W. J Mater Res 2002, 17, 940.
7. Bhimaraj, P.; Burris, D. L.; Action, J.; Sawyer, W. G.; Toney, C. G.; Siegel, R. W.; Schadler, L. S. Wear 2005, 258, 1437.
8. Rong, M. Z.; Zhang, M. Q.; Zheng, Y. X.; Zeng, H. M.; Friedrich, K. Polymer 2001, 42, 3301.
9. Hsiue, G. H.; Kuo, W. J.; Huang, Y. P.; Jeng, R. J. Polymer 2000, 41, 2813.

10. McCarthy, D. W.; Mark, J. E.; Schaefer, D. W. J Polym Sci Part B: Polym Phys 1998, 36, 1167.
11. García, M.; Vliet, G. V.; Cate, M. G. J. T. T.; Chávez, F.; Norder, B.; Kooi, B. J.; Zyl, W. E. V.; Verweij, H.; Blank, D. H. A. Polym Adv Technol 2004, 15, 164.
12. Silveira, K. F.; Yoshida, I. V. P.; Nunes, S. P. Polymer 1995, 36, 1425.
13. Ejaz, M.; Yamamoto, S.; Ohno, K.; Tsujii, Y.; Fukuda, T. Macromolecules 1998, 31, 5934.
14. Kim, J. B.; Bruening, M. L.; Baker, G. L. J Am Chem Soc 2000, 122, 7616.
15. Quirk, R. P.; Mathers, R. T.; Cregger, T.; Foster, M. D. Macromolecules 2002, 35, 9964.
16. Husemann, M.; Mecerreyes, D.; Hawker, C. J.; Hedrick, J. L.; Shah, R.; Abbott, N. L. Angew Chem Int Ed Engl 1999, 38, 647.
17. Schmidt, R.; Zhao, T. F.; Green, J. B.; Dyer, D. J. Langmuir 2002, 18, 1281.
18. Mansky, P.; Liu, Y.; Huang, E.; Russell, T. P.; Hawker, C. Science 1997, 275, 1458.
19. Lindenblatt, G.; Schartl, W.; Pakula, T.; Schmidt, M. Macromolecules 2000, 33, 9340.
20. Ranjan, R.; Brittain, W. J. Macromolecules 2007, 40, 6217.
21. Husseman, M.; Malmstrom, E. E.; McNamara, M.; Mate, M.; Mecerreyes, D.; Benoit, D. G.; Hedrick, J. L.; Mansky, P.; Huang, E.; Russell, T. P.; Hawker, C. J. Macromolecules 1999, 32, 1424.
22. Matyjaszewski, K.; Miller, P. J.; Shukla, N.; Immaraporn, B.; Gelman, A.; Luokala, B. B.; Siclovan, T. M.; Kickelbick, G.; Vallant, T.; Hoffmann, H.; Pakula, T. Macromolecules 1999, 32, 8716.
23. Yu, W. H.; Kang, E. T.; Neoh, K. G. Langmuir 2004, 20, 8294.
24. Perruchot, C.; Khan, M. A.; Kamitsi, A.; Armes, S. P.; von Werne, T.; Patten, T. E. Langmuir 2001, 17, 4479.
25. Li, C. Z.; Benicewicz, B. C. Macromolecules 2005, 38, 5929.
26. Baum, M.; Brittain, W. J. Macromolecules 2002, 35, 610.
27. Jones, D. M.; Brown, A. A.; Huck, W. T. S. Langmuir 2002, 18, 1265.
28. Parvole, J.; Laruelle, G.; Guimon, C.; Francois, J.; Billon, L. Macromol Rapid Commun 2003, 24, 1074.
29. Farmer, S. C.; Patten, T. E. Chem Mater 2001, 13, 3920.
30. von Werne, T.; Patten, T. E. J Am Chem Soc 2001, 123, 7497.
31. Li, D. J.; Jones, G. L.; Dunlap, J. R.; Hua, F. J.; Zhao, B. Langmuir 2006, 22, 3344.
32. Chen, X. Y.; Randall, D. P.; Perruchot, C.; Watts, J. F.; Patten, T. E.; von Werne, T.; Armes, S. P. J Colloid Interface Sci 2003, 257, 56.
33. Yu, H. J.; Luo, Z. H. J Polym Sci Part A: Polym Chem 2010, 49, 174.
34. Yu, H. J.; Luo, Z. H. Polym Eng Sci 2011, 51, 218.
35. Haller, I. J Am Chem Soc 1978, 100, 8050.
36. Zhang, K.; Li, H. T.; Zhang, H. W.; Zhao, S.; Wang, D.; Wang, J. Y. Mater Chem Phys 2006, 96, 477.
37. Ek, S.; Root, A.; Peussa, M.; Niinistö, L. Thermochim Acta 2001, 379, 201.
38. Vansant, E. F.; van der Voort, P.; Vroncken, K. C. Characterization and Chemical Modification of the Silica Surface; Elsevier: Amsterdam, 1995; p 135.
39. Yamaguchi, M.; Nakamura, Y.; Iida, T. Polym Polym Compos 1998, 6, 85.
40. Tanaka, S.; Kaihara, J.; Nishiyama, N.; Oku, Y.; Egashira, Y.; Ueyama, K. Langmuir 2004, 20, 3780.
41. Watts, J. F.; Wolstenholme J. An Introduction to Surface Analysis by XPS and AES; Wiley: Chichester, 2005; p 76.
42. Brinker, C. J.; Scherer, G. W. The Physics and Chemistry of Sol Gel Processing; Elsevier Science: London, 1990; p 108.
43. Mellon, V.; Rinaldi, D.; Bourgeat-Lami, E.; D'Agosto, F. Macromolecules 2005, 38, 1591.
44. Inoubli, R.; Dagréou, S.; Khoukh, A.; Roby, F.; Peyrelasse, J.; Billon, L. Polymer 2005, 46, 2486.
45. Han, Y.; Mayer, D.; Offenhäusser, A.; Ingebrandt, S. Thin Solid Films 2006, 510, 175.